INTERNATIONAL JOURNAL FOR NUMERICAL METHODS IN FLUIDS, VOL. 6, 819–839 (1986)

ANALYSIS OF LUBRICATED SQUEEZING FLOW

A. C. PAPANASTASIOU*, C. W. MACOSKO AND L. E. SCRIVEN

Department of Chemical Engineering and Materials Science, University of Minnesota, Minneapolis, MN 55455, U.S.A.

SUMMARY

A thin film of low-viscosity lubricating liquid between a solid wall and a viscous material reduces shear stress on the latter and tends to make it flow as though it were slipping along the wall. The result when the lubricated material is being squeezed out of the gap between approaching parallel plates is flow more nearly irrotational, or extensional, the more effective the lubricating film on the plates. Two Newtonian analyses of this flow situation are reported. One is an approximate, asymptotic analytical solution for Newtonian lubricating flow in the films and combined mixed flow, shear and extension, in the viscous layer. The second is a full two-dimensional axisymmetric solution of the momentum and continuity equations along with the kinematic condition which governs the motion of the interface. Both analyses indicate that there are two limiting flow regimes, depending on the ratio of the thickness of each of the two phases to radius and on the viscosity ratio of the two liquids. In one limit the flow is parallel squeezing and the lubricant layer slowly thins and persists a long time. In the other the lubricant is expelled preferentially. Implications of the results are discussed for rheological characterization of viscoelastic liquids and for prediction of lubricated or autolubricated flows in processing situations.

KEY WORDS Lubricated Flow Extensional Flow Compression Moulding Two-Liquid Interface Flow

INTRODUCTION

Extensional flows are common in nature and in technology. They are an essential part of many industrial processes: in coating operations as in the manufacture of photographic films and magnetic tapes, for example; in such polymer forming operations as blow moulding, vacuum forming, film blowing and foaming processes; and in lubricated and autolubricated flows of shear-thinning polymeric materials as in compression moulding. They are also of interest from the viewpoint of molecular theory because many non-Newtonian liquids behave differently in extension and shear.

At the same time extensional flows, in contrast to shear flows, which are rotational, are tough to create experimentally because of their irrotational character, which is inconsistent with the presence of solid boundaries or curved menisci.[1] Thus measurement of extensional material functions is still relatively undeveloped in comparison to shear rheometry.

Winter *et al.*[2] recently suggested that lubricated stagnation flow dies can be used to generate steady extensional flows. Van Aken and Janeschitz-Kriegl[3,4] used lubricated stagnation flow for generating equal biaxial extension. They reported birefringence and total thrust measurements on polystyrene. Macosko *et al.*[5] recently reported experimental results with a lubricated planar stagnation die.

* Present address: Department of Chemical Engineering, The University of Michigan, Dow Building, Ann Arbor, Michigan 48109-0135, U.S.A.

0271–2091/86/110819–21$10.50

Received 14 February 1986
Revised 18 April 1986

Chatraei *et al.*[6] found squeezing flow between two disks with lubricated surfaces, (Figure 1) to generate a homogeneous compression or equal biaxial extension in a high viscosity polymer sample. The apparatus was extremely simple: two steel disks with a central rod to align the sample and keep it from slipping off centre, a linear variable displacement transformer to measure displacement, and silicone oil bath. In a recent development the central rod and the oil bath have been eliminated.

For these experiments, however, there has been no rigorous mathematical analysis with which to evaluate whether the flow is close enough to irrotational to provide an adequate approximation. The data were analysed under the assumption that the flow was an ideal extensional one, despite the fact that the boundary conditions involved prevent this from being strictly true. The question remains to what extent the assumption is admissible. Pearson[7] studied some interesting special problems by applying the Couette flow approximation to thin lubricating layers. Joseph[8] proposed a slip boundary condition to account for a thin lubricating layer; however his analysis is limited to steady unidirectional flows in which the lubrication approximation can be applied to both phases. Macosko, *et al.*[5] discussed boundary conditions for lubricated flows and suggested various limiting conditions. Meyer[9] solved the Reynolds equation for flow in a thin lubrication layer with the method of lines and proved that the line-discretization solution converges to the solution of a variational inequality derived from the Reynolds equation. In a parallel, independent study Lee *et al.*[10] analysed compressive flow between parallel disks of Newtonian liquid when there is a transverse viscosity gradient in the liquid. They used the Galerkin/finite element method but did not describe the critical aspects of their implementation, although they discussed boundary conditions at the edge of the disks. Their results include cases of coextrusion of two Newtonian liquids of different viscosities, but when the two lubricating layers together are not thinner than the more viscous layer between them.

The objective here is a generally applicable theory of quasi-steady-state, creeping, two-liquid, axisymmetric radial flows of Newtonian liquids. The finite element treatment and the asymptotic

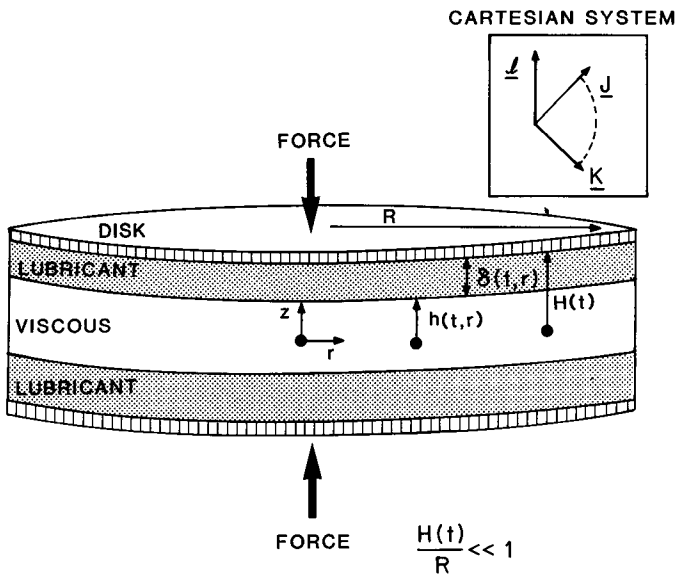

Figure 1. Lubricated squeezing flow. Two disks are pressed together by a constant squeezing force F; each moves with speed $v(t) = dH/dt$. The two liquids are forced out radially

analysis which follow apply directly or are readily extended to the flows encountered in the references of the last two paragraphs. One of the phases is always a thin lubrication layer. The interface of this layer evolves with time according to the kinematic condition at a free surface.[11] Across the interface shear stress is continuous and, although there are discontinuities of pressure and viscous normal stress, the total normal stress is continuous because interfacial tension effects are taken to be negligible. The thin lubrication layer is here supposed to remain thick enough that the thin-film and wetting effects, treated by Teletzke *et al.*[12] become unimportant.

Traction boundary conditions are imposed as natural ones[13] and velocity boundary conditions are imposed as essential ones. The unsteady character of the problem is brought about by a constant squeezing force applied externally to the solid boundaries. This force is represented by an integral boundary condition and is treated simultaneously with the other differential equations by the finite element method, as described below.

The results reveal that there are two limiting flow regimes that correspond to different ranges of the ratios of the thickness of the lubricating layer and viscous core layer to the disk radius and of the viscosity of the core liquid to that the less viscous lubricating liquid. Starting from these findings we construct approximate analytic solutions for the two limiting cases. In one the radial velocity peaks in the viscous layer and this is accompanied by predominantly Couette, or drag, flow in the lubricant film. In the other case the maximum of the radial velocity is in the lubricant layer, which moves in mainly Poiseuille, or pressure, flow. Many of the results were presented at the International Symposium on Interrelations between Processing Structure and Properties of Polymeric Materials, in Athens, 29 August–2 September 1982 (cf. Reference 14).

GOVERNING EQUATIONS AND BOUNDARY CONDITIONS

The flow configuration and co-ordinates are shown in Figure 1. Under a constant squeezing force F, a viscous Newtonian liquid is being squeezed out of the gap of thickness $H(t)$ between approaching parallel disks which are lubricated by a less viscous Newtonian liquid. Between the two immiscible Newtonian liquids is a non-planar axisymmetric interface at distance $h(r, t)$ from the midplane. The lubricant layers are of thickness $\delta(r, t) = H(t) - h(r, t)$, which is much less than $H(t)$. We solve the problem on just one quarter of the domain because of its axisymmetric character. Figure 2 shows the appropriate finite element domain as well as the boundary conditions, which are discussed below.

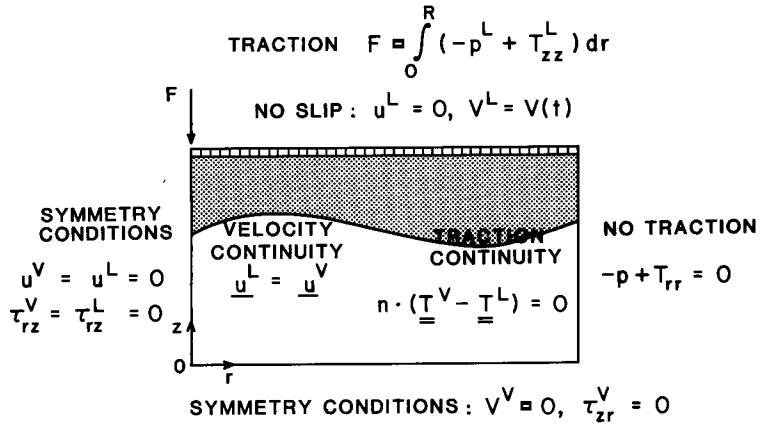

Figure 2 The boundary conditions. The constant squeezing force is distributed uniformly over each disk

Within each flowing liquid, mass and momentum must be conserved: for creeping, quasi-steady, incompressible flow and negligible effects of gravity this requires that in the viscous phase

$$\nabla\cdot\mathbf{u}^{V}=0, \qquad \nabla\cdot\mathbf{T}^{V}=\mathbf{0}. \tag{1}$$

and in the liquid phase

$$\nabla\cdot\mathbf{u}^{L}=\mathbf{0}, \qquad \nabla\cdot\mathbf{T}^{L}=\mathbf{0}. \tag{2}$$

$\mathbf{T}$ is the total stress tensor, defined for a Newtonian liquid as $\mathbf{T}=-p\mathbf{I}+\boldsymbol{\tau}=-p\mathbf{I}+\mu[\nabla\mathbf{u}+(\nabla\mathbf{u})^{T}]$, p being the pressure relative to that in the adjacent gas phase, and μ the viscosity of the liquid. That the quasi-steady creeping flow approximation is appropriate is born out by the results, as discussed below. The location $h(r,t)$ of the interface is an additional unknown field; the kinematic condition that the free surface remain a material surface provides the additional equation needed:

$$\frac{\partial h}{\partial t}+\mathbf{u}\cdot\nabla h=0. \tag{3}$$

So the only time derivative is in the kinematic condition (3), since time derivatives of velocity are negligible in the momentum equations under the quasi-steady state approximation.

The momentum equation requires boundary conditions on every boundary. These are summarized in Figure 2. At the midplane of symmetry there is neither normal velocity nor viscous shear stress. Along the z-axis of symmetry there is neither radial velocity nor shear stress. At the moving disks the normal velocity is uniform and the total normal stress integrated over the surface of the disk is equal to the squeezing force F. At the interface, surface tension effects are supposed to be negligible and so the viscous traction must be continuous:

$$\mathbf{n}\cdot(\mathbf{T}^{V}-\mathbf{T}^{L})=0. \tag{4}$$

The projections of this equation require that shear stress and normal stress be continuous:

$$\mathbf{tn}:(\mathbf{T}^{V}-\mathbf{T}^{L})=0, \quad \text{i.e. } T^{V}_{tn}-T^{L}_{tn}=0, \tag{5a}$$

$$\mathbf{nn}:(\mathbf{T}^{V}-\mathbf{T}^{L})=0, \quad \text{i.e. } T^{V}_{nn}-T^{L}_{nn}=0. \tag{5b}$$

Here t is the tangent unit vector to the interface and $\mathbf{n}$ is the normal unit vector to the interface. Velocity must also be continuous across the interface:

$$\mathbf{u}^{V}=\mathbf{u}^{L}. \tag{6}$$

At the outlet we take the normal stress to be negligible:

$$T^{V}_{nn}=T^{L}_{nn}=0. \tag{7}$$

Although this is strictly true only at the free surface of the liquid extruded from the gap between the disks as squeezing proceeds (and only when the capillary pressure of surface tension acting in the curved meniscus is negligible), the error introduced is small inasmuch as $H/R\ll 1$ and the velocity profile within the extrudate becomes uniform within a distance $r-R$ of the order of H. (The situation when the gap is not much less than the disk radius is treated by Lee *et al.*[10] We impose no boundary condition on the shear stress at the outlet and instead require that the x-component of the momentum equation holds within the domain and at the boundary $r=R$. The effects of these boundary conditions on the results are described below.

The motion of the disk toward the fixed midplane is governed by Newton's second law:

$$M\frac{\mathrm{d}^{2}H}{\mathrm{d}t^{2}}=-(W+Mg)+\int_{0}^{R}2\pi r\,T^{L}_{nn}|_{z=H}\,\mathrm{d}r,$$

where M is the mass of the disk, W is the weight of the applied load on it and $T^L_{nn}|_{z=H}$ is the normal stress exerted on the disk by the lubricant. We suppose that the motion is slow, i.e. $W + Mg \gg M(\mathrm{d}^2H/\mathrm{d}t^2)$, so that the boundary condition is

$$F = W + Mg = \int_0^R 2\pi r T^L_{nn}|_{z=H}\,\mathrm{d}r, \tag{8}$$

along with the condition of no slip

$$\begin{aligned} \mathbf{e}_r\cdot\mathbf{u}^L &= 0, \\ \mathbf{e}_z\cdot\mathbf{u}^L &= -v(t) = \mathrm{d}H/\mathrm{d}t. \end{aligned} \tag{9}$$

Here $v(t)$ is the uniform normal speed of the disk with respect to the midplane, which responds as a function of time to the constant squeezing force $F = W + Mg$.

Dimensionless forms

The governing equations and boundary conditions are made dimensionless by choosing convenient units of length (R), stress ($\tau_0 \equiv F/\pi R^2$) and velocity ($\tau_0 R/2\mu_V$):

$$\begin{aligned} &z^* = z/R, \quad r^* = r/R, \quad h^* = h/R, \quad p^* = p/\tau_0, \quad \boldsymbol{\tau}^* = \boldsymbol{\tau}/\tau_0, \\ &\mathbf{u}^* = (2\mu_V/\tau_0 R)\mathbf{u}, \quad t^* = t(2\mu_V/\tau_0 R)/R. \end{aligned} \tag{10}$$

The resulting dimensionless equations, with asterisks suppressed here and hereafter, are

$$\nabla\cdot\mathbf{u}^V = 0, \quad \nabla\cdot\mathbf{T}^V = \mathbf{0}, \quad \mathbf{T}^V = -p^V\mathbf{I} + \tfrac{1}{2}[\nabla\mathbf{u}^V + (\nabla\mathbf{u}^V)^T], \tag{1*}$$

$$\nabla\cdot\mathbf{u}^L = 0, \quad \nabla\cdot\mathbf{T}^L = \mathbf{0}, \quad \mathbf{T}^L = -p^L\mathbf{I} + \frac{1}{2}\left(\frac{\mu_L}{\mu_V}\right)[\nabla\mathbf{u}^V + (\nabla\mathbf{u}^V)^T], \tag{2*}$$

$$\frac{\partial h}{\partial t} + \mathbf{u}\cdot\nabla h = 0, \tag{3*}$$

$$\mathbf{n}\cdot(\mathbf{T}^V - \mathbf{T}^L) = \mathbf{0}, \tag{4*}$$

$$T^V_{tn} - T^L_{tn} = 0, \quad T^V_{nn} - T^L_{nn} = 0, \tag{5*}$$

$$\mathbf{u}^V = \mathbf{u}^L, \tag{6*}$$

$$T^V_{nn} = T^L_{nn} = 0, \tag{7*}$$

$$2\pi\int_0^1 T^L_{nn}|_{z=H}\, r\,\mathrm{d}r = 1, \tag{8*}$$

$$\mathbf{e}_r\cdot\mathbf{u}^L = 0, \quad \mathbf{e}_z\cdot\mathbf{u}^L \equiv -v(t) = \mathrm{d}H/\mathrm{d}t. \tag{9*}$$

The units chosen preserve the continuity of the dimensionless velocities at the interface ((3*) and (6*)) and facilitate programming the computations in the two phases, which then differ solely by the viscosity ratio ((1*) and (2*)).

FINITE ELEMENT FORMULATION

The finite element formulation of free surface problems is well described elsewhere.[11,15] Here we merely outline the procedure, emphasizing those parts of the formulation that relate to the interface and to the axisymmetric character of the flow.

In the Galerkin/finite element method, the unknown velocity components, pressure and interface location are expanded in a suitable set of finite element basis functions, ϕ^i and ψ^i:

$$\begin{aligned} u(r,z,t) &= \sum u_i(t)\phi^i\{\xi(r,z),\eta(r,z)\},\\ v(r,z,t) &= \sum v_i(t)\phi^i\{\xi(r,z),\eta(r,z)\},\\ p(r,z,t) &= \sum p_i(t)\psi^i\{\xi(r,z),\eta(r,z)\},\\ h(r,t) &= \sum h_i(t)\phi^i\{\xi(r,z),\eta(r,z=h)\}\\ &= \sum h_i(t)\phi^i\{\xi(r,z),\eta=-1 \quad \text{or} \quad \eta=1\}. \end{aligned} \tag{11}$$

Here ξ and η are Cartesian co-ordinates in a basic square $Q=\{\xi,\eta/-1\leqslant\xi\leqslant 1,-1\leqslant\eta\leqslant 1\}$ from which each of the subdomains or elements of the actual flow is mapped through an isoparametric relation in order to accommodate the irregular boundaries and to reduce computational cost, as compared to finite difference discretization. Hence $\phi^i(\xi,\eta)$ and $\psi^i(\xi,\eta)$ are prescribed axisymmetric functions defined only on the basic square Q. They are shown in Figure 3. The basis functions $\phi^i(\xi,\eta=-1$ or $\eta=1)$ in which interface position is expanded are the one-dimensional functions $\phi^i(\xi,\eta)$ evaluated at $\eta=-1$ for elements adjacent to the interface on the side of the lubricant phase, and at $\eta=1$ for elements adjacent to the interface on the side of the viscous phase. The coefficients $u_i(t), v_i(t), p_i(t)\, h_i(t)$ are the values of the unknowns at the nodes of the elements and are determined by substituting the expansions (11) in (1*) to (3*) and integrally weighted the residuals, i.e. the amounts by which these equations fail to be satisfied, with each of the basis functions. By requiring these weighted residuals to vanish, the residuals themselves are made orthogonal to the finite-dimension function space spanned by the basis functions: e.g. $M_i=\int_V(\nabla\cdot\mathbf{T})\phi^i\,dV=0$. For the axisymmetric problem at hand, V, the domain in which the equations are solved, extends from 0 to 1 in the radial direction, from 0 to $H(t)/R$ to $H(t)/R$ in the lubricant layer, and from 0 to π in the θ-direction.

The Galerkin weighted residuals of the continuity equation in the viscous and the lubricant layers are, respectively

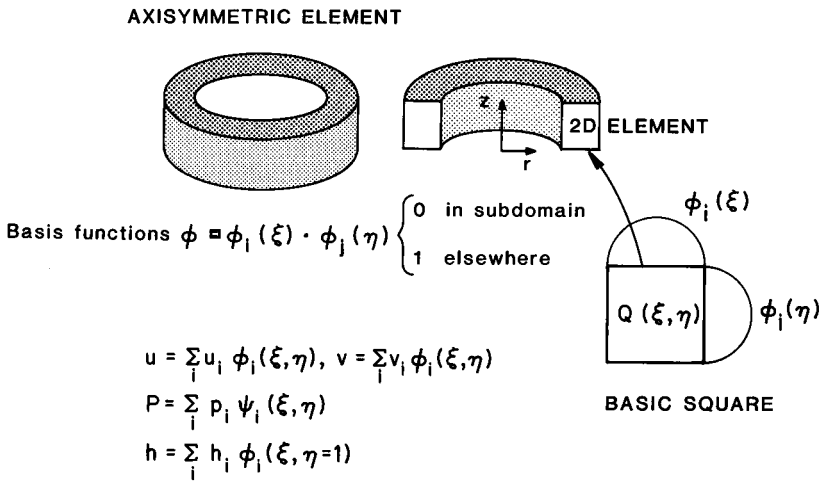

Figure 3. The tessellation into axisymmetric finite elements and the biquadratic basis functions ϕ_i

$$C_{i,\mathrm{V}} = \int_0^{\pi}\int_0^{1}\int_0^{h(r,t)/R} (\nabla\cdot\mathbf{u}^{\mathrm{V}})\psi^i \,\mathrm{d}V = \pi\int_0^{1}\int_0^{h(r,t)/R} (\nabla\cdot\mathbf{u}^{\mathrm{V}})\psi^i r\,\mathrm{d}r\,\mathrm{d}z = 0,$$

$$C_{i,\mathrm{L}} = \int_0^{\pi}\int_0^{1}\int_{h(r,t)/R}^{H(t)/R} (\nabla\cdot\mathbf{u}^{\mathrm{L}})\psi^i \,\mathrm{d}V = \pi\int_0^{1}\int_{h(r,t)/R}^{H(t)/R} (\nabla\cdot\mathbf{u}^{\mathrm{L}})\psi^i r\,\mathrm{d}r\,\mathrm{d}z = 0. \tag{12}$$

The Galerkin weighted residuals of the momentum equation are broken into two parts with the divergence theorem:

$$M_i = \iiint_V (\nabla\cdot\mathbf{T})\phi^i \,\mathrm{d}V = -\iiint_V (\nabla\phi^i\cdot\mathbf{T})\,\mathrm{d}V + \int_A (\mathbf{n}\cdot\mathbf{T})\phi^i \,\mathrm{d}A = 0.$$

$\mathbf{n}$ is the outward pointing normal to the boundary; $\mathbf{n}_{\mathrm{I}}$ is the normal to the interface. Thus for the viscous layer the Galerkin weighted residuals are

$$\mathbf{M}_i^{\mathrm{V}} = \underbrace{\int_0^{\pi}\int_0^{1}\int_0^{h/R} (\nabla\phi^i\cdot\mathbf{T}^{\mathrm{V}})r\,\mathrm{d}r\,\mathrm{d}\theta\,\mathrm{d}z}_{\text{Viscous Layer}} - \underbrace{\int_0^{\pi}\int_0^{1} (\mathbf{n}_{\mathrm{I}}\cdot\mathbf{T}^{\mathrm{V}})\phi^i r\,\mathrm{d}r\,\mathrm{d}\theta}_{\text{Interface}} - \underbrace{\int_0^{\pi}\int_0^{1} (-\mathbf{e}_z\cdot\mathbf{T}^{\mathrm{V}})\phi^i|_{z=0} r\,\mathrm{d}r\,\mathrm{d}\theta}_{\text{Midplane}}$$

$$- \underbrace{\int_0^{\pi}\int_0^{h/R} (\mathbf{e}_r\cdot\mathbf{T}^{\mathrm{V}})\phi^i|_{r=1}\,\mathrm{d}\theta\,\mathrm{d}z}_{\text{Exit}} - \underbrace{\int_0^{1}\int_0^{h/R} (-\mathbf{e}_\theta\cdot\mathbf{T}^{\mathrm{V}}|_{\theta=0} + \mathbf{e}_\theta\cdot\mathbf{T}^{\mathrm{V}}|_{\theta=\pi})\,\mathrm{d}r\,\mathrm{d}z}_{\text{Plane Through } z\text{-Axis}} = \mathbf{0}. \tag{13}$$

Projected onto orthogonal directions $\mathbf{i}, \mathbf{k}$ and $\mathbf{l}$, shown in Figure 1, equation (13) has components which, after being integrated over θ, are

$$M_{i,j}^{\mathrm{V}} = \mathbf{j}\cdot\mathbf{M}_i^{\mathrm{V}} = 0, \tag{13a}$$

$$M_{i,k}^{\mathrm{V}} = \mathbf{k}\cdot\mathbf{M}_i = \int_0^{1}\int_0^{h/R}\left[\frac{\partial\phi^i}{\partial r}\tau_{rz}^{\mathrm{V}} + 2\frac{\partial\phi_i}{\partial z}(-p^{\mathrm{V}} + \tau_{rr}^{\mathrm{V}}) + \phi^i\left(-\frac{-p^{\mathrm{V}} + \tau_{\theta\theta}^{\mathrm{V}}}{r}\right)\right] r\,\mathrm{d}r\,\mathrm{d}z$$

$$- \int_0^{1} (\mathbf{k}\cdot\mathbf{n}_{\mathrm{I}}\cdot\mathbf{T}^{\mathrm{V}})\phi^i r\,\mathrm{d}r + \int_0^{1} (\mathbf{k}\cdot\mathbf{e}_z\cdot\mathbf{T}^{\mathrm{V}})\phi^i|_{z=0}\, r\,\mathrm{d}r - \int_0^{h/R} (\mathbf{k}\cdot\mathbf{e}_r\cdot\mathbf{T}^{\mathrm{V}})\phi^i|_{r=1}\,\mathrm{d}z = 0, \tag{13b}$$

$$M_{i,l}^{\mathrm{V}} = \mathbf{l}\cdot\mathbf{M}_i^{\mathrm{V}} = \int_0^{1}\int_0^{h/R}\left[\frac{\partial\phi^i}{\partial r}\tau_{rz}^{\mathrm{V}} + 2\frac{\partial\phi_i}{\partial z}(-p^{\mathrm{V}} + \tau_{zz}^{\mathrm{V}})\right] r\,\mathrm{d}r\,\mathrm{d}z$$

$$- \int_0^{1} (\mathbf{l}\cdot\mathbf{n}_{\mathrm{I}}\mathrm{p}\cdot\mathbf{T}^{\mathrm{V}})\phi^i r\,\mathrm{d}r + \int_0^{1} (\mathbf{l}\cdot\mathbf{e}_z\cdot\mathbf{T}^{\mathrm{V}})\phi^i|_{z=0} r\,\mathrm{d}r - \int_0^{h/R} (\mathbf{l}\cdot\mathbf{e}_r\cdot\mathbf{T}^{\mathrm{V}})\phi^i|_{r=1}\,\mathrm{d}z = 0. \tag{13c}$$

The identities $\mathbf{e}_r \equiv \mathbf{j}\sin\theta + \mathbf{k}\cos\theta$, $\mathbf{e}_z \equiv \mathbf{l}$, $\mathbf{e}_\theta|_{\theta=0} = -\mathbf{e}_\theta|_{\theta=\pi} = -\mathbf{k}$, $\int_0^{\pi}\sin\theta\,\mathrm{d}\theta = +2$, and $\int_0^{\pi}\cos\theta\,\mathrm{d}\theta = 0$, have been made in (13). The second term of (13b) is the tangential traction of the liquid on the interface and is balanced by that exerted by the lubricant layer as expressed in (5b). The third term is the tangential traction on the midplane of symmetry, $z = 0$, and is zero. The fourth term is the normal traction at the exit, which vanishes by (7). The second term of (13c) is the normal traction on the interface and is balanced by that of the lubricant layer. The third term is the normal traction on the midplane of symmetry and is not known *a priori*; however, the equation that requires the momentum residual to vanish over each subdomain around a node on the midplane is replaced by the essential boundary condition $\mathbf{e}_z\cdot\mathbf{u}^{\mathrm{V}} = 0$.

Similar equations of vanishing momentum weighted residuals are generated for the lubricant layer and its boundaries. The domain of integration extends from 0 to 1 in the r-direction, from

$h(r,t)/R$ to $H(t)/R$ in the z-direction and from 0 to π in the θ-direction. The equations that require the r-momentum and z-momentum residuals to vanish over each subdomain around a node on the plate are replaced by the essential boundary conditions $\mathbf{e}_r \cdot \mathbf{u}^L = 0$ and $\mathbf{e}_z \cdot \mathbf{u}^L = -v(t)$, respectively. At just one of these nodes the latter condition is replaced by the overall force balance (8*). The equation that requires the r-momentum residuals to vanish over each subdomain around a node on the z-axis is replaced by the essential boundary condition $\mathbf{e}_r \cdot \mathbf{u}^L = 0$.

At the interface the velocity and the traction must be continuous. This is ensured by requiring the corresponding velocity coefficients u_i and v_i in the two phases to be identical at common nodes on the interface. In contrast, pressure is allowed to be discontinuous by assigning distinct pressure coefficients p_i^L and p_i^V at those nodes. Figure 4 shows the arrangement of the unknown coefficientss in elements adjacent to the interface, and the basic square $Q(\xi,\eta)$ which is isoparametrically mapped into these elements.

The evolution of the flow with time is dictated by the kinematic equation (3*), which is discretized by forward differencing to give

$$\frac{h^{(n+1)} - h^{(n)}}{\Delta t} + \mathbf{u}^{(n)} \cdot \nabla h^{(n)} = 0. \tag{14a}$$

This equation is then weighted with the biquadratic basis functions $\phi^i(\xi, -1)$ in cases of elements in the lubricant layer adjacent to the interface and $\phi^i(\xi, 1)$ in cases of elements in the viscous phase there:

$$\int_0^{2\pi} \int_0^1 \left[\frac{h^{(n+1)} - h^{(n)}}{\Delta t} + \mathbf{u}^{(n)} \cdot \Delta h^{(n)} \right] \phi^i r \mathrm{d}r \mathrm{d}\theta = 0. \tag{14b}$$

These equations are solved simultaneously with those of continuity residuals (12) and momentum residuals (13).

The domain was tessellated into 76 quadrilateral elements; biquadratic basis functions were used to approximate velocity and bilinear ones to approximate pressure. The initially unknown location of the interface was approximated by the same biquadratic basis functions, but evaluated at the interface (indeed at $\eta = -1$ or $\eta = 1$ through the isoparametric mapping). For comparable accuracy small quadrilateral elements were found necessary near the outlet, where the boundary conditions change from 'no slip' to 'no traction'. The tessellation is shown in Figure 5. As the two disks approached each other this tessellation was rearranged with time in such a way that the ratio of the z-co-ordinates of an element to that of the interface remained constant. The Galerkin weightings—momentum equations with biquadratics, continuity equations with bilinears and kinematic equations with quadratics—resulted in a linear system of 859 linear equations in as many unknowns. Apart from the integral boundary condition from the squeezing force, the matrix of this large system is almost banded. To solve it we used a modified[16] frontal solver.[17]

The derivatives and integrals in equation (13) and in their counterparts for the lubricant layer, and in equation (14b) were evaluated in the basic square $Q(\xi,\eta)$ and on its boundary, through the isoparametric mapping $r = \sum_1^q r_i \phi^i(\xi,\eta)$, $z = \sum_1^q z_i(h) \phi^i(\xi,\eta)$, which maps $Q(\xi,\eta)$ into each of the 76 quadrilaterals. Here r_i and $z_i(h)$ are the co-ordinates of the nodes; $z_i(h)$ is a function of the interface elevation h because the tessellation deforms in the z-direction with the interface. Further details of this process, e.g. the isoparametric mapping and the transformations of derivatives and integrals appear elsewhere.[11,13,15]

The computations were started from an initial rest state $\{\mathbf{u} = \mathbf{v} = \mathbf{p} = \mathbf{0}, \mathbf{h}_{(r)}^0, \mathbf{H}^{(0)}\}$. The initial configuration of the interface, $h(r)$, need not have been parallel to the disks, but in what follows the interface was a plane $h^{(0)}$ parallel to the disks unless otherwise stated. At time $t = 0$ the constant

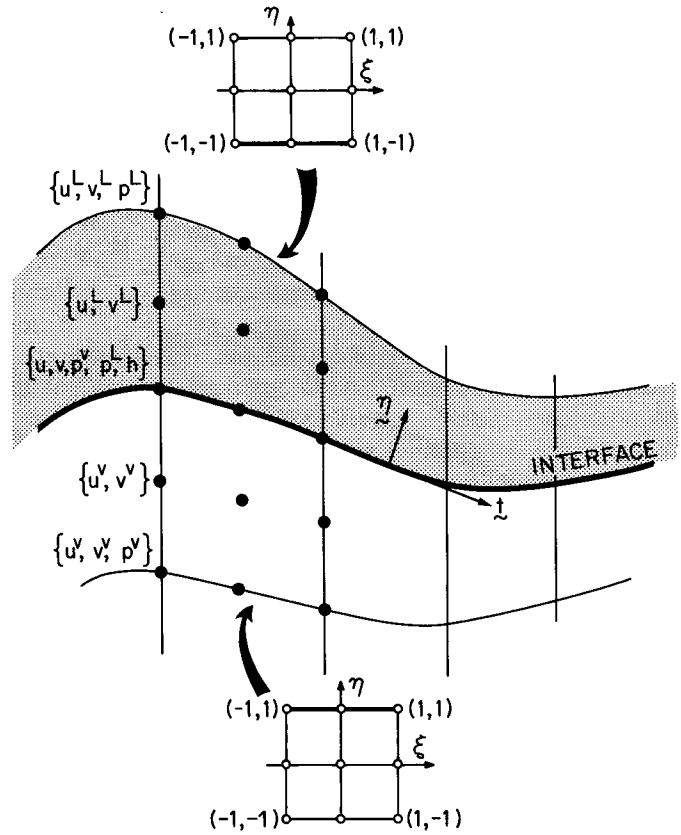

Figure 4. Isoparametric mapping of basic square $Q(\xi\, n)$ into elements adjacent to the interface

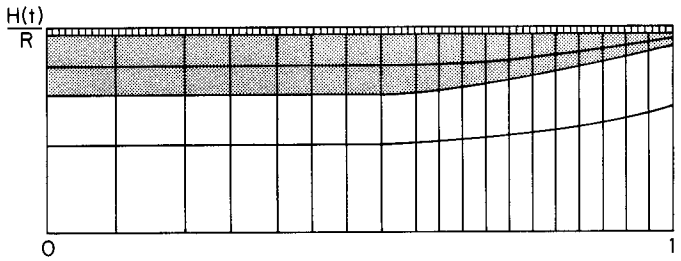

Figure 5. The finite element tessellation in the meridional plane: 4 × 19 quadrilateral elements, which result in 859 nodal unknowns

squeezing force was applied and the set $\{\mathbf{u}^{(0)}, \mathbf{v}^{(0)}, \mathbf{p}^{(0)}, \mathbf{h}^{(1)}, \mathbf{H}^{(1)}\}$ was computed after time $(\Delta t)_1$. The tessellation was then updated with the newly found nodal values $h = h_i$ and $H = H_i$ and the set $\{\mathbf{u}^{(1)}, \mathbf{v}^{(1)}, \mathbf{p}^{(1)}, \mathbf{h}^{(2)}, \mathbf{H}^{(2)}\}$ after time $(\Delta t)_2$ was computed. In the matrix form $\mathbf{Ax} = \mathbf{b}$,

$$\begin{bmatrix} \mathbf{M}_k^{\mathrm{V}} & \mathbf{M}_k^{\mathrm{V}} & \mathbf{M}_k^{\mathrm{V}} & 0 & 0 & 0 & 0 & 0 \\ \mathbf{M}_l^{\mathrm{V}} & \mathbf{M}_l^{\mathrm{V}} & \mathbf{M}_l^{\mathrm{V}} & 0 & 0 & 0 & 0 & 0 \\ \mathbf{C}^{\mathrm{V}} & \mathbf{C}^{\mathrm{V}} & 0 & 0 & 0 & 0 & 0 & 0 \\ \mathbf{K} & \mathbf{K} & 0 & \mathbf{K} & \mathbf{K} & \mathbf{K} & 0 & 0 \\ 0 & 0 & 0 & 0 & \mathbf{M}_k^{\mathrm{L}} & \mathbf{M}_k^{\mathrm{L}} & \mathbf{M}_k^{\mathrm{L}} & 0 \\ 0 & 0 & 0 & 0 & \mathbf{M}_l^{\mathrm{L}} & \mathbf{M}_l^{\mathrm{L}} & \mathbf{M}_l^{\mathrm{L}} & 0 \\ 0 & 0 & 0 & 0 & \mathbf{C}^{\mathrm{L}} & \mathbf{C}^{\mathrm{L}} & 0 & 0 \\ 0 & 0 & 0 & 0 & 0 & \mathbf{B}^{\mathrm{L}} & 0 & \mathbf{B}^{\mathrm{L}} \end{bmatrix} \begin{bmatrix} \mathbf{u}_{\mathrm{V}}^{(n)} \\ \mathbf{v}_{\mathrm{V}}^{(n)} \\ \mathbf{p}_{\mathrm{V}}^{(n)} \\ \mathbf{h}^{(n+1)} - \mathbf{h}^{(n)} \\ \mathbf{u}_{\mathrm{L}}^{(n)} \\ \mathbf{u}_{\mathrm{L}}^{(n)} \\ \mathbf{p}_{\mathrm{L}}^{(n)} \\ \mathbf{H}^{(n+1)} - \mathbf{H}^{(n)} \end{bmatrix} = \begin{bmatrix} \text{B.C. 1} \\ \text{B.C. 2} \\ 0 \\ 0 \\ \text{B.C. 3} \\ \text{B.C. 4} \\ 0 \\ 0 \end{bmatrix}, \tag{15}$$

where $\mathbf{M}_{\mathrm{p}}^{\mathrm{G}}$ is the matrix of coefficients of the p-component of the momentum weighted residual equation of the G-layer, equations (13); $\mathbf{C}^{\mathrm{G}}$ is the matrix of coefficients of the continuity equation of the G-layer, equation (12); $\mathbf{K}$ is the matrix of coefficients of the kinematic equation weighted residuals, equation (14b); $\mathbf{B}^{\mathrm{L}}$ is the matrix of coefficients of the kinematic equation (9); B.C. 1 are the essential boundary conditions at the z-axis, $u = 0$; B.C. 2 are the essential boundary conditions at the midplane, $v = 0$; B.C. 3 are the essential boundary conditions at the plate and at the z-axis, $u = 0$; B.C. 4 are the essential boundary conditions at the plate, $v = v(t)$ and $\{\mathbf{u}^{(n)}, \mathbf{v}^{(n)}, \mathbf{p}^{(n)}, \mathbf{h}^{(n)}, \mathbf{H}^{(n)}\}$ are vectors of the nodal unknowns at time $(\Delta t)_n$, e.g. $u^{(n)} = \{u_1^{(n)}, u_2^{(n)}, \ldots, u_N^{(n)}\}$, $\mathbf{v}^{(n)} = \{v_1^{(n)}, v_2^{(n)}, \ldots, v_N^{(n)}\}$, etc.

The choice of the time step Δt in this forward difference scheme is crucial to avoiding excessive computation cost. Analysis of numerical stability based on a spectral radius of the amplification matrix[18,19] $\mathbf{A}$, under the assumption of planar interface, i.e. $\partial h/\partial r = 0$, showed that the forward difference scheme gives a stable non-oscillatory solution if

$$E = \left| \Delta t \left(\left. \frac{\partial v^{\mathrm{L}}}{\partial H} \right|_{z=H} + \left. \frac{\partial v}{\partial h} \right|_{z=h} \right) \right| < 1. \tag{16}$$

The time step Δt was continuously updated according to the computed derivatives in (16) so that $E = 0{\cdot}8$. The number and the size of the time steps depend on the magnitude of the squeezing force and the viscosity ratio. In general small time steps were required initially (0·01 s) and fairly large time steps afterwards (0·5 s). A typical run took 100 time steps.

ASYMPTOTIC ANALYSIS

The finite element results described in the next section showed that for an initially planar interface there are two limiting flow regimes; these are diagrammed in Figure 6. When $\mu_{\mathrm{L}} R^2/\mu_{\mathrm{V}}\delta^2 \gg 1$,

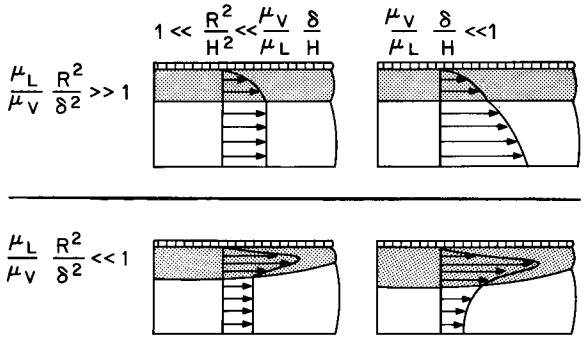

Figure 6. The two limiting flow regimes that are predicted by finite element analysis depend on the dimensionless group $\mu_{\mathrm{L}} R^2/\mu_{\mathrm{V}}\delta^2$

where δ is the lubricant thickness $\delta(t,r) \equiv H(t) - h(r,t)$, the interface remains planar and the maximum radial velocity is in the viscous layer. When $\mu_L R^2/\mu_V \delta^2 \ll 1$ the interface attains a slightly parabolic shape, the lubricant is encapsulated between the rigid approaching disk and the highly viscous material, and the velocity maximum occurs in the lubricant layer. For these two limiting flow regimes we constructed approximate analytic solutions guided by the qualitative features of the finite element solutions. Although the dimensionless group $\mu_L R^2/\mu_V \delta^2$ was chosen on the basis of a series of results of Galerkin/finite element analyses, its mathematical origin and physical significance are illuminated by dimensional analysis of the governing equations and boundary conditions, as is shown in the Appendix.

The case $\mu_L R^2/\mu_V \delta^2 \gg 1$: parallel squeezing

The interface remains planar and the velocity maximum is in the viscous layer. We then seek Stefan-type[20] similarity solutions, which satisfy the momentum and continuity equations, of the form

$$u^L = ar(z^2 - H^2),$$
$$u^V = r(b - cz^2), \tag{17}$$

where a, b and c are constants. The ratio of the extension rate, $\dot{\varepsilon} = \partial u^V/\partial r = b - cz^2$, to the shear rate, $\dot{\gamma} = \partial u^V/\partial z = -2rcz$, controls the b/c ratio. If $b \gg cH^2$ the flow is virtually extensional and if $b \ll cH^2$ the flow is mixed, dominated by shear. The boundary conditions (5a) and (6) are sufficient to determine the three constants. The solution is then

$$u^L(t,r,z) = \frac{v(t) r \mu_V}{4H^3\left(\dfrac{\delta(t)\mu_V}{H(t)\mu_L} + \dfrac{1}{3}\right)\mu_L}[H^2(t) - z^2], \tag{18a}$$

$$u^V(t,r,z) = \frac{v(t) r}{4H^3\left(\dfrac{\delta(t)\mu_V}{H(t)\mu_L} + \dfrac{1}{3}\right)}\left[\frac{\mu_V}{\mu_L} 2H(t)\delta(t) + h^2(t) - z^2\right], \tag{18b}$$

where $v(t)$ is the speed with which one disk approaches the other. Plainly the flow in the viscous layer is a controllable mixture of shear and extension: all that need be adjusted is the 'mobility ratio' $\delta\mu_V/H\mu_L$. Equation (18a) reduces to the Stefan[21] and Reynolds[21] equation when a single layer is squeezed, i.e. in the limit $\delta = 0$. It reduces to ideal extensional flow in the limit $\delta\mu_V/H\mu_L \gg \frac{1}{3}$.

The pressure distributions in the two layers are found by integrating the momentum equations (1) and (2) and applying boundary conditions (5b) and (7):

$$p^L(t,r,z) = \frac{2v(t)\mu_V}{4H^3\left(\dfrac{\delta(t)\mu_V}{H(t)\mu_L} + \dfrac{1}{3}\right)}\left[3\frac{\mu_V}{\mu_L} 2H(t)\delta(t) + \frac{R^2 - r^2}{2}\right], \tag{18c}$$

$$p^V(t,r,z) = \frac{2v(t)\mu_V}{4H^3\left(\dfrac{\delta(t)\mu_V}{H(t)\mu_L} + \dfrac{1}{3}\right)}\left[\frac{\mu_V}{\mu_L} 2H(t)\delta(t) + \frac{R^2 - r^2}{2} - (h^2(t) - z^2)\right]. \tag{18d}$$

The squeezing force F can be calculated from (8):

$$F = \frac{\pi v(t) R^2 \mu_V}{2H^3\left(\dfrac{\delta(t)\mu_V}{H(t)\mu_L} + \dfrac{1}{3}\right)}\left[\frac{R^2}{4} + 6\frac{\mu_V}{\mu_L}H(t)\delta(t)\right]. \tag{18e}$$

This force can be made proportional to the viscosity of the lubricant by making the gap far smaller than the disk radius and the mobility ratio high, i.e. by arranging that $R^2/H^2 \gg \delta\mu_V/H\mu_L \gg \frac{1}{3}$. It reduces to the Stefan squeezing force in the limit $\delta = 0$. Equation (18e) agrees with the one proposed by Lee *et al.*[10] for a thin lubrication layer, i.e. for $\delta/H \ll 1$.

The evolution of the lubricant layer thickness $\delta(t)$ is found by solving the Reynolds equation in the lubricant layer:

$$\frac{1}{r}\frac{\partial}{\partial r}\left[\frac{r\delta^3(t)}{12\mu_L}\frac{\partial p^L}{\partial r} - v\mu_V\frac{\delta(t)}{2}\right] = \frac{\partial\delta(t)}{\partial t}. \tag{18f}$$

The solution, under the assumption that the interface remains planar, is

$$\frac{\delta(t)}{\delta_0} = -\frac{3}{4}\frac{\mu_L}{\mu_V}\frac{H(t)}{H_0} + \left[\left(\frac{3}{4}\frac{H(t)}{H_0}\frac{\mu_L}{\mu_V}\right)^2 + \frac{H(t)}{H_0}\right]^{1/2}. \tag{18g}$$

The plate separation $H(t)$ follows from (18e) and (18g). It is

$$\frac{H_0^{1/2}}{\delta_0}\left(\frac{1}{H^{3/2}} - \frac{1}{H_0^{3/2}}\right) - 16\frac{\mu_V}{\mu_L R^2}\ln\left(\frac{H(t)}{H_0}\right) = \frac{16Ft}{3\pi\mu_L R^4}. \tag{18h}$$

When $\mu_V\delta_0 H_0/\mu_L R^2 \gg 1$ the equation reduces to

$$\frac{H(t)}{H_0} = \exp\left(-\frac{F}{3\pi R^2\mu_V}t\right), \tag{18i}$$

which represents an ideal extensional deformation.[22]

The case $\mu_L R^2/\mu_V\delta^2 \ll 1$: nearly extensional flow

The interface attains a slightly parabolic shape and the velocity maximum is in the lubricant layer. Therefore we seek slowly varying solutions, which satisfy the momentum and continuity equations and the no slip boundary conditions, of the form

$$u^V = G(r)(1 + z^2 d),$$

$$u^L = F(r)[z^2 - z(H + h) + Hh] + G(r)(1 + h^2 d)\frac{z - H}{h - H}. \tag{19}$$

The flow in the lubricant consists of a Poiseuille flow represented by the first term, and of a drag or Couette flow induced by the viscous layer, represented by the second term. The separability of the r and z dependences of u_r^V is indicated by the finite element results. Substituting (19) into (5a) and (6), eliminating $G(r)$, and applying boundary conditions (5b) and (7) yields the solution

$$u^V(t, r, z) = v(t)\left[\frac{1}{8}\frac{\mu_L}{\mu_V}\frac{H(t)}{\delta(t)}\frac{r^3}{H^3(t) - h^3(t)} + \frac{r}{2H(t)}\right]\left[1 + 6\frac{\mu_L}{\mu_V}\frac{H(t)}{\delta(t)}\frac{z^2}{H^2(t) - h^2(t)}\right], \tag{20a}$$

$$u^{L}(t,r,z) = -v(t)\left[\frac{9}{4}\frac{\mu_L}{\mu_V}\frac{H(t)}{\delta(t)}\frac{r^3}{H(t)\delta^4(t)}\right][z^2 - z[H(t)+h(t)] + H(t)h(t)] + u^{V}\frac{z-H(t)}{h(t)-(t)}, \tag{20b}$$

$$p^{V}(t,r,z) = \frac{v(t)\mu_V}{H(t)}\left[1 + 6\frac{\mu_L}{\mu_V}\frac{H(t)}{\delta(t)}\frac{R^2-r^2}{H^2(t)-h^2(t)}\right], \tag{20c}$$

$$p^{L}(t,r,z) = \frac{v(t)\mu_V}{H(t)}\left[3 + \frac{8}{9}\left(\frac{\mu_L^2 H(t)}{\mu_V^2\delta(t)}\right)\frac{R^4-r^4}{\delta^4}\right], \tag{20d}$$

$$F = \frac{3\pi v(t)\mu_V R^2}{H(t)} + \int_0^R \frac{16\pi v(t)\mu_L^2(r^4-R^4)}{9\mu_V\delta^5} r\,dr. \tag{20e}$$

The evolution of the lubricant layer thickness $\delta(t)$ is found by solving the Reynolds equation in the lubricant layer,

$$-\frac{1}{r}\frac{\partial}{\partial r}\left(r\int_{h(t)}^{H(t)} u^{L}\,dz\right) = \frac{\partial\delta(t)}{\partial t}. \tag{21a}$$

The solution to (21a), provided the interface is almost planar, i.e. $\partial\delta/\partial r \approx 0$, is

$$\frac{\frac{3}{2}\frac{\mu_L}{\mu_V}r^2 + \frac{\delta^3(t,r)}{H}}{\frac{3}{2}\frac{\mu_L}{\mu_V}r^2 + \frac{\delta_0^3}{H_0}} = \left(\frac{H}{H_0}\right)^{1/2}. \tag{21b}$$

The plate separation $H(t)$, for negligible $3\mu_L r^2/2\mu_V$, follows from (21b) and (20e). It is

$$\ln\left(\frac{H(t)}{H_0}\right) - \frac{32\mu_L^2 R^4 H_0^{5/2}}{243\mu_V^2\delta_0}\left[\frac{1}{H(t)^{3/2}} - \frac{1}{H_0^{3/2}}\right] = \frac{Ft}{3\pi\mu_V R^2}. \tag{21c}$$

The qualitative features of equation (21c) are shown in Figure 7. Both equations (21c) and Figure 7 show that an almost ideal extensional flow persists until the second term of the equation becomes significant.

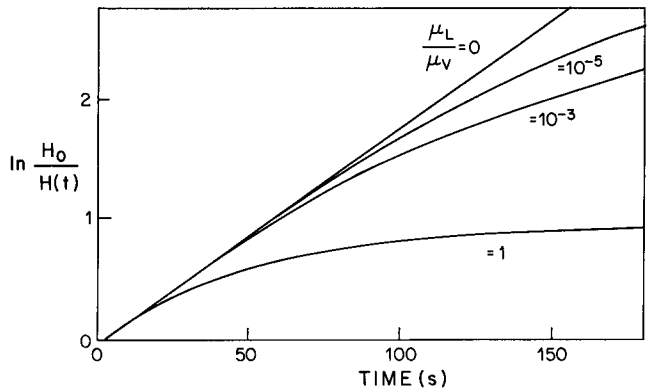

Figure 7. The evolution of the disk separation as predicted by the asymptotic solution, equation (21c), for the conditions $F/A = 2540$ Pa, $\delta_0/H_0 = 0{\cdot}5$ mm/7·85 mm and $R/H_0 = 25{\cdot}4$ mm/9·35 mm

In the limit $\mu_L r^2/\mu_V \delta^2(t) \ll 1$, equations (20a), (20c) and (20e), reduce to the ideal extension forms

$$u^V = \frac{v(t)r}{2H(t)}, \tag{22a}$$

$$p^V = \frac{v(t)\mu_V}{H(t)}, \tag{22b}$$

$$F = \frac{3\pi v(t)\mu_V R^2}{H(t)}, \tag{22c}$$

$$\frac{H(t)}{H_0} = \exp\left(-\frac{Ft}{3\pi R^2 \mu_V}\right). \tag{22d}$$

The extension rate is then $\dot{\varepsilon} = \partial u/\partial r = v(t)/2H(t)$ and by virtue of (22c) is a constant: $\dot{\varepsilon} = F/6\pi R^2 \mu_V$. Thus steady ideal extensional flow is approached under these conditions.

In the work reported here we have not investigated whether the solutions found are stable to flow disturbances. Instead we rely on the available experimental data[22] and on the finite element results which show that they do have a domain of stability: Figure 8 shows that, starting from any of the interface profiles shown there, a parabolic profile is always attained shortly after the application of the squeezing force.

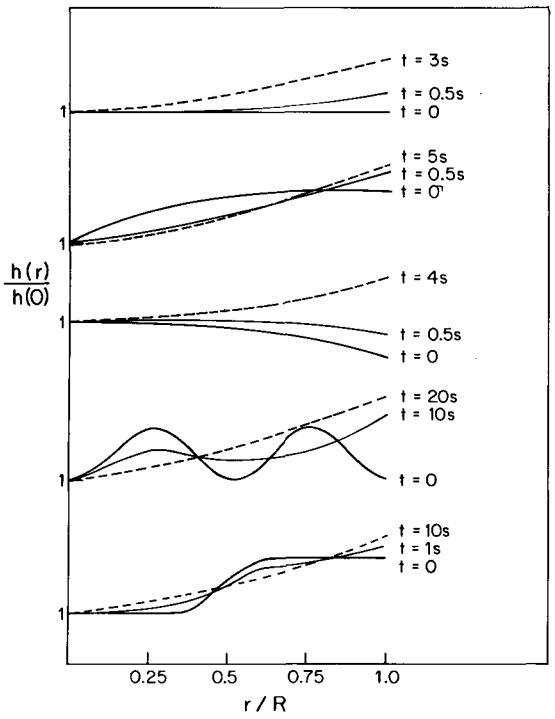

Figure 8. Computer-generated finite element predictions of the interface evolution starting from different initial configurations

RESULTS AND DISCUSSION

To validate the results of the finite element analysis we first tested them against the asymptotic analysis of squeezing flow in a single layer. This analysis is due to Stefan.[20] Figure 9 compares radial velocities, pressure distribution and evolution of the thickness. The pressure distribution disagrees by as much as 10 per cent near the outlet; the cause is the natural boundary condition (7) as opposed to a vanishing pressure in Stefan's asymptotic analysis. When the viscosities of the two layers are identical the results from two-layer squeezing flow calculations agree in the same way with Stefan's asymptotic solution. The effects of changing the boundary condition at the outlet are indicated in Figure 10, which shows the pressure and centre-plane radial velocity in the last few elements at the outflow. Three kinds of boundary conditions are examined. One is vanishing of the pressure at the outlet ($p = 0$). Another is vanishing of the total normal stress at the outlet (equation (7)). A third option is no boundary condition on the normal stress at the outlet, requiring instead that the r-component of the Galerkin weighted residual of the momentum equation hold in the subdomain and at its boundary $r = R$. (As described on p. 000

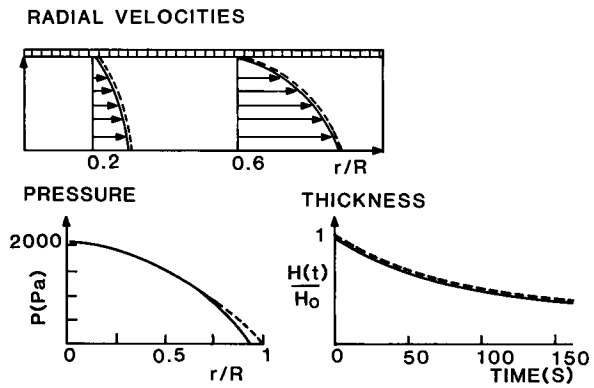

Figure 9. Computer-generated finite element predictions of squeezing flow of a single layer, compared with Stefan's[20] asymptotic analysis (– –)

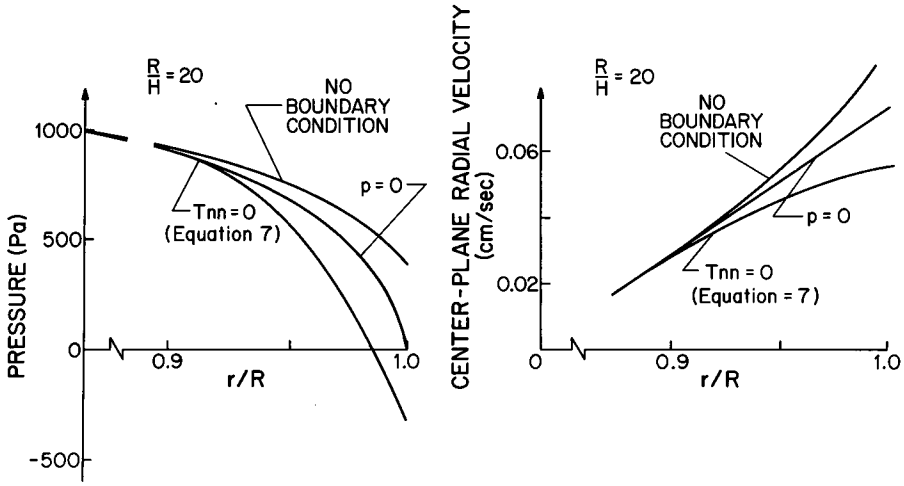

Figure 10. The effects of different outlet boundary conditions on the pressure and centre-plane radial velocity

the shear stress at the outlet was invariably treated this way.) The results show that the choice of the boundary conditions at the outlet affects the flow only locally within a distance $R = r$ of the order of H. These effects are vanishingly small inasmuch as $H/R \ll 1$.

In Figure 11 the predictions for two-layer flow are shown for the case $\mu_L R^2/\mu_V \delta^2 \gg 1$. Both finite element results and asymptotic analysis show that the flow in the viscous phase is closer to extensional, the smaller the viscosity ratio μ_L/μ_V, and reduces to the conventional parabolic flow when this ratio is unity, as shown in Figure 9. The flow in the lubricant is mostly induced by drag of the flowing viscous layer. However, there is a small amount of pressure-driven or Poiseuille flow as well, neglect of which in the asymptotic analysis would violate the boundary conditions at the interface (conditions 5(a) and (6)). The pressure in both phases is relatively low, as predicted by both finite element and asymptotic analysis. The pressure is discontinuous at the interface according to the equation (5b), but the pressure gradient is continuous. The interface remains planar, the lubricant thickness decreases uniformly with time, and the lubricant persists for a long time. The squeezing force is proportional to the viscosity of the lubricant for $R^2/H^2 \gg \mu_V \delta/\mu_L H \gg 1$.

Predictions for the other limiting case, $\mu_L R^2/\mu_V \delta^2 \ll 1$ are shown in Figure 12. Again finite element results agree with the asymptotic solution. There is some disagreement in the lubricant layer near the outlet because the assumption $\mu_L r^2/\mu_V \delta^2 \ll 1$ starts to fail. The interface does not remain planar any more. It curves, encapsulating the lubricant, and a pressure dominated flow is induced. The radial velocity has a profound maximum within the lubricant layer. The

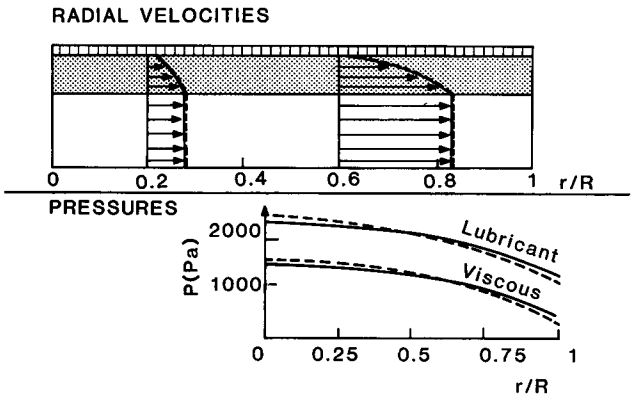

Figure 11. Computer-generated finite element predictions in the case $\mu_L R^2/\mu_V \delta^2 = 5$ and $R^2/H^2 = 25$ are well approximated by the asymptotic solution (– – –)

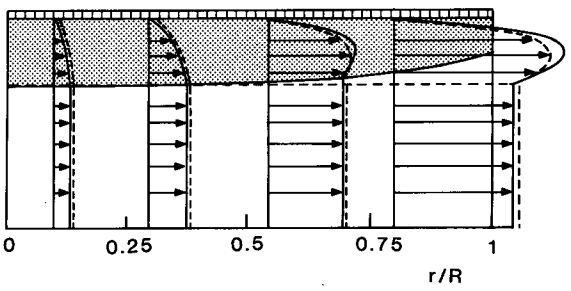

Figure 12. Computer-generated finite element predictions in the case $\mu_L R^2/\mu_V \delta^2 = 0{\cdot}1$ and $R^2/H^2 = 25$ are well approximated by the asymptotic solution (– –), except near the exit (see text)

squeezing force is proportional to the viscosity of the viscous layer and the flow in that layer approaches an extensional, irrotational one.

In both limiting cases the accelerations d^2H/dt^2 and $\partial v/\partial t$ can be evaluated from the results and prove to be negligible in the parameter ranges of interest:

$$\frac{\mu_L}{\mu_V}\frac{R^2}{\delta^2} \geqslant 10 \begin{cases} \max\left|\dfrac{d^2H}{dt^2}\right| \simeq 10^{-3}\,\mathrm{cm\,s^{-2}}, & \dfrac{F}{M} \simeq 10^{3}\,\mathrm{cm\,s^{-2}}, \\ \max\left|\dfrac{\partial u^L}{\partial t}\right| \simeq 10^{-4}\,\mathrm{cm\,s^{-2}}, & \left|\dfrac{\mu_L}{\rho_L}\dfrac{\partial^2 u^L}{\partial r^2}\right| \simeq 10^{-2}\,\mathrm{cm\,s^{-2}}, \end{cases}$$

$$\frac{\mu_L}{\mu_V}\frac{R^2}{\delta^2} \leqslant 0{\cdot}1 \begin{cases} \max\left|\dfrac{d^2H}{dt^2}\right| \simeq 10^{-2}\,\mathrm{cm\,s^{-2}}, & \dfrac{F}{M} \simeq 10^{3}\,\mathrm{cm\,s^{-2}}, \\ \max\left|\dfrac{\partial u^L}{\partial t}\right| \simeq 10^{-3}\,\mathrm{cm\,s^{-2}}, & \left|\dfrac{\mu_L}{\rho_L}\dfrac{\partial^2 u^L}{\partial r^2}\right| \simeq 10^{-1}\,\mathrm{cm\,s^{-2}}. \end{cases}$$

Thus the quasi-steady creeping flow approximation is entirely justified.

Figure 13 shows that the time course of disk separation under a constant squeezing force, as measured by Chatraei[22], is predicted satisfactorily by both finite element and asymptotic analysis.

In Figure 14 the lubricant pressure, which was measured at four different radial positions after a steady-state was achieved, is plotted along with finite element predictions and the asymptotic approximation. Again the finite element results agree with the experiments throughout the flow domain, apart from the measurement near the centre which was affected by the presence of a central rod used to align the sample and keep it from slipping off-centre. The asymptotic solution fails near the outlet, i.e. near the disk circumference, because the assumption $\mu_L r^2/\mu_V\delta^2 \ll 1$, on which it rests, starts to fail there.

In Figure 15 the evolution of the lubricant pressure at the second radial position is plotted. The finite element predictions agree with the experiments. The asymptotic solution slightly overestimates these results.

Finally, in Figure 16 the extension rate $\dot{\varepsilon} = [1/Ht]\,dH(t)/dt$ calculated by Chatraei[22], who assumed an ideal extensional flow in the viscous layer, is plotted along with finite element predictions and the asymptotic approximation. A steady extension, $\dot{\varepsilon} =$ constant, is reached after a short start-up of 20 s. Whereas the finite element predictions agree throughout with these

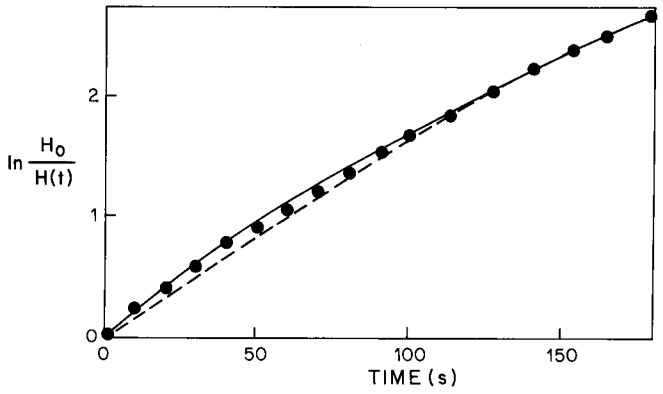

Figure 13. The evolution of the disk separation as measured by Chatraei *et al.*[6] (●) and as predicted by the finite element analysis (——) and by the equation (21c) (——), for the condition $\mu_L/\mu_V = 0{\cdot}45$ pa s/270,000 Pa s; $R/H_0 = 25{\cdot}4$ mm/9.35 mm and $\delta_0/H_0 = 0{\cdot}5$ mm/9·35 mm

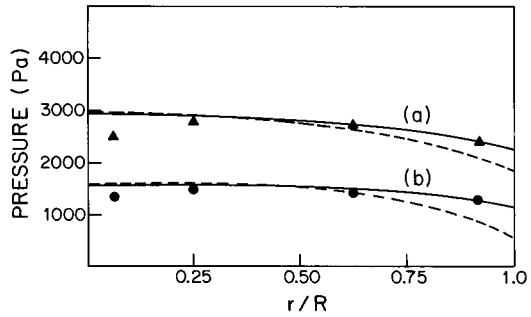

Figure 14. The lubricant pressure distribution as measured by Chatraei[22] (●) and as predicted by the finite element analysis (——) and by the asymptotic solution (——), for the conditions (a) $\mu_L/\mu_V = 0{\cdot}45$ Pa s/27,000 Pa s, $R/H_0 = 25{\cdot}4$ mm/7·85 mm, $\delta_0/H_0 = 0{\cdot}5$ mm/7·85 mm and $F/A = 2540$ Pa; (b) $\mu_L/\mu_V = 0{\cdot}45$ Pa s/27,000 Pa s, $R/H_0 = 25{\cdot}4$ mm/9·35 mm, $\delta_0/H_0 = 0{\cdot}5$ mm/9·35 mm and $F/A = 1340$ Pa

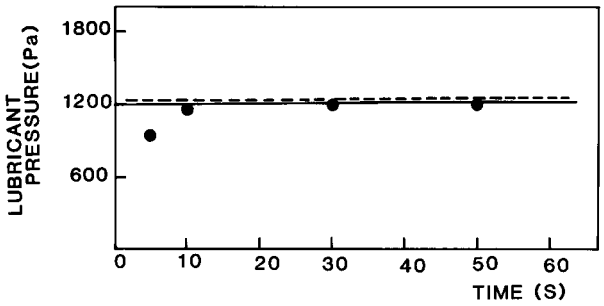

Figure 15. The evolution of the lubricant pressure at the second radial position of Figure 12, as measured by Chatraei[22] (●), and as predicted by the finite element analysis (——) and by the asymptotic solution (——), for the conditions $\mu_L/\mu_V = 0{\cdot}45$ Pa s/27,000 Pa s, $R/H_0 = 25{\cdot}4$ mm/7·85 mm, $\delta_0/H_0 = 0{\cdot}5$ mm/7.85 mm and $F/A = 2540$ Pa

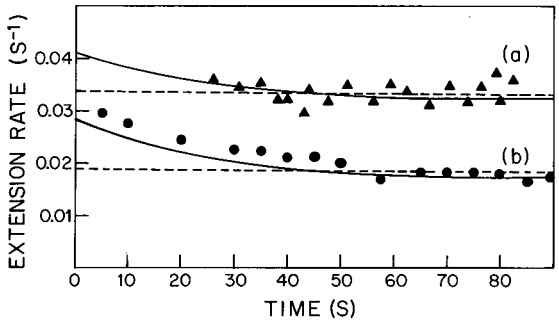

Figure 16. Extension rates, as calculated by Chatraei[22], and as predicted by the finite element analysis (——) and by the asymptotic solution (——), for the conditions (a) $\mu_L/\mu_V = 0{\cdot}45$ Pa s/27,000 Pa s, $R/H_0 = 25{\cdot}4$ mm/7·85 mm, $\delta_0/H_0 = 0{\cdot}5$ mm/7·85 mm and $F/A = 1340$ Pa; (b) $\mu_L/\mu_V = 0{\cdot}45$ Pa s/27,000 Pa s, $R/H_0 = 25{\cdot}4$ mm/9·35 mm, $\delta_0/H_0 = 0{\cdot}5$ mm/9·35 mm and $F/A = 2540$ Pa

experimental findings, the asymptotic solution fails within the start-up period but does predict the final steady extension rate that was measured.

CONCLUSION

The methods of subdomains and Galerkin weighted residuals together with the extremely convenient finite element basis functions (in this case second degree polynomials for velocity, first degree for pressure) permitted accurate analysis of the axisymmetric, time dependent flow of multiple layers of Newtonian liquid, including the pressure discontinuity at the free interfaces between layers and the integrated traction boundary condition. The qualitative features of the results suggested two limiting flow regimes, for which approximate solutions were constructed in closed form. For these limiting cases the predictions computed with the aid of finite element basis functions agree with the closed-form solutions, and both agree with the available experimental data.

Both the computer-aided finite element analysis and closed form asymptotic solutions indicate that controllably mixed flows can be achieved with the lubricated squeezing method. Shear dominates over extension in these flows when the viscosities of the two liquids are of the same order of magnitude. But the ideal, irrotational extensional flow is closely approached in the core liquid when its viscosity is more than 100 times that of thin lubricating layers on both of the approaching disks.

The dimensionless group $\mu_L R^2/\mu_V \delta^2$, where δ is lubricant film thickness and R is the radius of disk, characterizes the flow in the lubricant. When $\mu_L R^2/\mu_V \delta^2 \gg 1$, drag flow of Couette type is induced in the lubricant by the relatively faster moving viscous phase. When $\mu_L R^2/\mu_V \delta^2 \ll 1$, pressure flow of Poiseuille type is induced in the lubricant, which lies between an approaching rigid disk and the almost stationary viscous phase. The squeezing force is also defined by the same dimensionless group.

The steady ideal extensional flow is well approximated whenever $\mu_L R^2/\mu_V \delta^2$ is much less than unity. In this case the ratio $v(t)/H(t)$ is constant and hence so also is the extension rate $\dot{\varepsilon} = \dot{H}(t)/H(t) = v(t)/H(t)$. Thus under these conditions the constant-force, lubricated squeezing flows would appear to be ideal for extensional measurements.

The chief limitations of lubricated squeezing flows as a means of characterizing non-Newtonian liquids are two; one experimental and one theoretical. Only a few highly viscous materials have been tested so far and whether the technique can be made to work on lower viscosity materials remains to be established. From the theoretical point of view, there is a need of regorous mathematical theory and computer methodology to treat what may be more complex flows when viscoelastic materials that require modern integral constitutive equations are to be characterized.[23]

ACKNOWLEDGEMENTS

This research was supported by grants-in-aid from the Xerox Foundation, the 3M Company and the University of Minnesota Graduate School and Computer Centre.

APPENDIX: THE DIMENSIONLESS PARAMETER $\mu_L R^2/\mu_V \delta^2$

To scale the radial components of the momentum equations (1) and (2) and interface conditions (5) in the usual way to permit comparison of the orders of magnitude of terms in the limiting cases of interest, the appropriate units of length are R in the radial direction in both layers and δ and H-δ in

the axial direction in the lubricant layer (L) and viscous layer (V), respectively. Then with v the unit of velocity and $\mu_V v/R$ the unit of pressure the equations are

$$\mu_V \frac{v}{R^2}\frac{\partial p_L^*}{\partial r^*} = \mu_L v\left(\frac{1}{R^2}\frac{\partial^2 u_L^*}{\partial r^{*2}} + \frac{1}{\delta^2}\frac{\partial^2 u_L^*}{\partial z^{*2}} - \frac{u_L}{R^2 r^{*2}}\right), \tag{23}$$

$$\mu_V \frac{v}{R^2}\frac{\partial p_V^*}{\partial r^*} = \mu_V v\left(\frac{1}{R^2}\frac{\partial^2 u_V^*}{\partial r^{*2}} + \frac{1}{(H-\delta)^2}\frac{\partial^2 u_V^*}{\partial z^{*2}} - \frac{u_V}{R^2 r^{*2}}\right), \tag{24}$$

$$\mu_L v\left(\frac{1}{\delta}\frac{\partial u_L^*}{\partial z^*} + \frac{1}{R}\frac{\partial v_L^*}{\partial r^*}\right) = \mu_V v\left(\frac{1}{H-\delta}\frac{\partial u_V^*}{\partial z^*} + \frac{1}{R}\frac{\partial v_V^*}{\partial r^*}\right), \tag{25}$$

$$-\mu_V \frac{v}{R} p_L^* + 2\mu_L \frac{v}{\delta}\frac{\partial v_L^*}{\partial z^*} = -\mu_V \frac{v}{R} p_V^* + 2\mu_V \frac{v}{H-\delta}\frac{\partial v_V^*}{\partial z^*}. \tag{26}$$

The variables are of order unity, so that under the circumstances that $\delta^2/H^2 \ll 1$ (thin lubricant layer) and $H^2/R^2 \ll 1$ (small gap-to-flow distance ratio, a condition for the lubrication approximation), the terms multiplied by each can be neglected. The remaining terms define a lubrication-type approximation (asterisks are suppressed here and hereafter):

$$\frac{\partial p_L}{\partial r} = \frac{\mu_L}{\mu_V}\frac{R^2}{\delta^2}\frac{\partial^2 u^L}{\partial z^2}, \tag{27}$$

$$\frac{\partial p_V}{\partial r} = \frac{R^2}{(H-\delta)^2}\frac{\partial^2 u_V}{\partial z^2}, \tag{28}$$

$$\frac{\partial u_L}{\partial z} = \frac{\mu_V \delta}{\mu_L (H-\delta)}\frac{\partial u_V}{\partial z}, \tag{29}$$

$$-p_L = -p_V. \tag{30}$$

Plainly the flow in the two layers is controlled by the dimensions groups $\mu_L R^2/\mu_V \delta^2$ and $\mu_V \delta/\mu_L (H-\delta) \approx \mu_V \delta/\mu_L H$ inasmuch as $R/(H-\delta) \gg 1$ in the situations treated above.

For a given pressure gradient $\partial p_L/\partial r$, which is mainly set by the external squeezing force according to the boundary conditions (8) at the moving plate, the flow in the lubricant layer is controlled by the dimensionless group $\mu_L R^2/\mu_V \delta^2$: if $\mu_L R^2/\mu_L \delta^2 \gg 1$ then $\partial^2 u_L/\partial z^2$ is small and the flow approaches the Couette type ('parallel squeezing'); if $\mu_L R^2/\mu_V \delta^2 \ll 1$ then $\partial^2 u_L/\partial z^2$ is large and the flow approaches the Poiseuille limit ('nearly extensional flow'). The sigificance of the other dimensionless groups, $\mu_V \delta/\mu_L H$, is obvious from equations (18a)–(18e) and (20a)–(20e).

REFERENCES

1. B. G. Higgins and L. E. Scriven, 'Interfacial shape and evolution equations for liquid films and other viscocapillary flows', *Ind. Eng. Chem. Fundam.*, **18**, 208–215 (1979).
2. H. H. Winter, C. W. Macosko and K. E. Bennett, 'Orthogonal stagnation flow, a framework for steady extensional flow experiments ', *Rheol. Acta*, **18**, 323–334 (1979).
3. J. A. van Aken and H. Janeschitz-Kriegl, 'New apparatus for the simultaneous measurement of stresses and flow birefringence in biaxial extension on polymer melts', *Rheol. Acta*, **19**, 744–752 (1980).
4. J. A. van Aken, and H. Janeschitz-Kriegl, 'simultaneous measurement of transient stress and flow birefringence in one-sided compression (biaxial extension) of polymer melt', *Rheol. Acta*, **20**, 419–432 (1981).
5. C. W. Macosko, M. A. Ocansey and H. H. Winter, 'Steady planar extension with lubricated dies', *J. Non-Newtonian Fluid Mech.*, **11**, 301–316 (1982).
6. S. Chatraei, C. W. Macosko and H. H. Winter, 'Lubricated squeezing flow: a new biaxial extensional rheometer', *J. Rheology*, **34**, 433–443 (1981).

7. J. R. A. Pearson, 'On the melting of solids near a hot moving interface, with particular reference to beds of granular polymers', *Int. J. Heat Mass Transfer*, **19**, 405–411 (1976).
8. D. D. Joseph, 'Boundary conditions for thin lubrication layers', *Phys. Fluids*, **23**, 2356–2358 (1980).
9. G. H. Meyer, 'An analysis of the method of lines for the reynolds equation in hydrodynamic lubrication', *SIAM J. Numer. Anal.*, **18**, 165–177 (1981).
10. S. J. Lee, M. M. Denn M. J. Crochet and A. B. Metzner, 'Compressive flow between parallel disks', *J. Non-Newtonian Fluid Mech.*, **10**, 3–30 (1982).
11. H. S. Kheshgi and L. E. Scriven, 'Penalty finite element analysis of unsteady free surface flow', in J. T. Oden *et al.* (eds), *Finite Elements in Fluids*, vol. **5**, Wiley, New York, 1983.
12. G. F. Teletzke, H. T. Davis and L. E. Scriven, 'Wetting hydrodynamics', *J. Fluid Mech.*, submitted.
13. S. F. Kistler and L. E. Scriven, 'Coating flows', in J. R. A. Pearson and S. M. Richardson (eds), *Computational Analysis of Polymer Processing*, Applied Science Publishers Ltd., London and New York, 1983.
14. A. C. Papanastasiou, C. W. Macosko and L. E. Scriven, 'Lubricated squeezing flow: computer simulation and asymptotic analysis', in J. C. Seferis and P. S. Theocaris (eds), *Proceedings of International Symposium on Interrelations between Processing Structure and Properties of Polymeric Materials*, Elsevier Scientific Publishing Company, Amsterdam, The Netherlands, 1985.
15. S. F. Kistler and L. E. Scriven, 'Coating flow theory by finite element and asymptotic analysis of the Navier–Stokes systems', *Int. j. numer. methods fluids*, **4**, 207–228 (1984).
16. A. C. Papanastasiou, 'Coating flows and rheology of viscoelastic materials', *Ph.D. Thesis*, University of Minnesota, Minneapolis, 1984.
17. P. Hood, 'Frontal solution program for unsymmetric matrices', *Int. j. numer. methods eng.*, **10**, 379–393 (1974).
18. A. C. Hindmarsh, and P. M. Gresho, *The Stability of Explicit Euler Time-Integration for Certain Finite Difference Approximations of the Multi-Dimensional Advection-Diffusion Equation*, Lawrence Livermore National Laboratory, Livermore, CA, 1983.
19. K. W. Morton, 'Stability of finite difference approximations to a diffusion-convection equation', *Int. j. numer. methods eng.*, **15**, 677–683 (1980).
20. M. J. Stefan, 'Versuche über die Scheinbare Adhäsion ', *Akad. Wissensch. Wien, Math.-Natur.*, **69**, 713–735 (1874).
21. O. Reynolds, 'On the theory of lubrication and its application to Mr. Beauchamp Tower's experiments including an experimental determination of the viscosity of olive oil', *Philos. Trans. R. Soc. Lond.*, **177**, 157–203 (1886).
22. S. Chatraei, 'Lubricated squeezing flow: a new biaxial extensional rheometer', *M. S. Thesis*, University of Minnesota, Minneapolis, 1981.
23. A. C. Papanastasiou, L. E. Scriven and C. W. Macosko, 'An integral constitutive equation for mixed flows: viscoelastic characterization', *J. Rheology*, **27**, 387–410 (1983).